

Wide Stopband Single Layer Quasi-Elliptic Ultra-Wideband Bandpass Filter

Muhammad Riaz, Bal S. Virdee, Dion Mariyanayagam, and Pancham Shukla

Abstract— This paper presents the design of a microstrip ultra-wideband (UWB) bandpass filter that exhibits desirable characteristics of low-loss, high selectivity, wide stopband and high out-of-band rejection at room temperature. These characteristics are normally achieved with high temperature superconductor filters that require cryogenic cooling. The design of the proposed filter was realized by exciting multiple resonant modes in a unique Z-shaped microstrip resonator. The admittance of the filter configuration can be tuned prior to fabrication to adjust its center frequency by about 11.5% without affecting the profile of the bandpass response however this can have an impact of the loss. The proposed configuration allows adjustment of the upper and lower transmission zeros defining the bandpass response by 20.5% and 11.4%, respectively, without degrading the overall filter response. The low-loss quasi-elliptic function UWB bandpass filter design was fabricated on a commercially available dielectric substrate using standard PCB technology and its performance verified. The fabricated filter exhibits insertion-loss of 0.68 dB and return-loss better than 17 dB.

Index Terms — Ultra-wideband (UWB) frequency discriminating devices, filters, multimode resonators.

I. INTRODUCTION

THE application of ultra-wideband (UWB) technology has become popular ever since the Federal Communications Commission (FCC) authorized the frequency band of 3.1–10.6 GHz for unlicensed use [1]. The restricted transmit power of -41dBm/MHz has undeterred the expansion of this technology. This is because UWB systems offer numerous advantages including better immunity to multipath propagation and narrowband interferences, higher data rate transmission, good penetration in materials, and smaller antenna size. These advantages have made it highly attractive for various applications including wireless communications, RFID, radar, and medical imaging.

In 2014, the European Union (EU) issued a directive on electromagnetic compatibility (EMC) that prohibits EM emissions from equipment that fall outside their normal operational frequency range. The purpose of this directive is to prevent adverse interference with other electronic systems, especially safety critical systems. This has made the bandpass filter (BPF) a key component of the RF front-end in the UWB system. Although UWB communication systems have

achieved an unprecedented improvement since being authorized by FCC for commercial use, however, it is still challenging to design a compact and high-performance UWB BPF that satisfies the FCC spectral mask. Because of the low emissions by UWB systems it is found from literature that the researchers and RF designers are mainly concerned about the bandwidth and size of the UWB filter with scant regard to the band-edge selectivity and out-of-band performance. Hence, even though the unwanted out-of-band emission power is relatively low it can still cause electromagnetic interference on other sensitive equipment. In practice, the out-of-band emissions can be mitigated by cascading the UWB filter with a band notch frequency discriminating device. This is not a desirable solution as it increases the overall dimensions and costs of RF front-end in the UWB system and leads to additional insertion-loss.

Various techniques and topologies have been explored to design UWB bandpass filters. Examples of recent UWB bandpass filters developed include high-temperature superconductors (HTS) realized by loading inside a quintuple-mode ring resonator with a pair of stepped-impedance open stubs [2]. Unwanted modes generated by this structure are suppressed using parallel-coupled lines with stepped-impedance ports. In [3] the UWB filter is implemented with a multiple-mode resonator (MMR) comprising a stepped impedance resonator (SIR) loaded with a rectangular stepped impedance stub. Low impedance line section of the SIR is connected to two horizontal high impedance sections on its two sides, which are parallel coupled to the input/output ports. In [4] a quintuple-mode HTS UWB filter is realized by loading three pairs of open stubs on the dual-ring resonator. Multiple modes are generating to create the passband response by tweaking the electrical length and impedance ratio of the stepped-impedance lines. The input/output ports are parallel coupled to the MMR. The UWB filter in [5] is made of two layers of substrate integrated waveguide (SIW) structures. The filter consists of a ridge SIW resonator inside the SIW waveguide and an impedance transformer. Examples of other UWB filter structures investigated to date can be found in references [6]-[13].

This paper describes the design of an ultra-wide bandpass filter that has characteristics of a quasi-elliptic response, flat group delay, high out-of-band rejection, and wide stopband at room temperature. The filter design is based on a z-shaped multi-mode resonator which can be easily implemented on a single layer of dielectric substrate. Moreover, the proposed filter does not require short-circuited vias or a defected ground-plane making it relatively easy to fabricate. The proposed structure excites even and odd-mode resonances that combine to create the required passband. The highly selective UWB filter is shown to have a relatively low insertion-loss

Dr M. Riaz now with the Dept. of Electrical Engineering, Grand Charter College of Engineering and Technology, Lahore, Pakistan.

Prof. B. S. Virdee, Dr P. Shukla & D. Mariyanayagam are at Center of Communications Technology, School of Computing and Digital Media, London Metropolitan University, London, UK.

(e-mail: ranariaz@yahoo.com and b.virdee@londonmet.ac.uk)

and high return-loss. These characteristics are normally attributed to UWB filters based on high-temperature superconductors. Unlike HTS filters the proposed filter does not require cryogenic cooling. It was fabricated on a commercially available standard dielectric substrate and its performance validated through measurement.

II. ANALYSIS OF THE PROPOSED UWB FILTER

The UWB response is created using a microstrip resonator structure shown in Fig.1 which resembles z-shaped cross with radial stub ends. The horizontal section of the cross includes three high impedance open-circuited stubs in the shape of an “E” that are outward facing and whose function is to provide a wide stopband above and below the passband. The center pin of the “E” stub is inter-digitally coupled to the input/output feedlines to reduce the in-band insertion-loss. The section forming the z-shaped structure is folded as shown simply to minimize the lateral dimension of the filter.

The central horizontal stepped impedance transmission-line section of the resonator is represented with characteristic admittance and length of Y_1, θ_1 , and Y_2, θ_2 , respectively; and the characteristic admittance and length of the lateral stepped impedance stub at the center are Y_3, θ_3 , and Y_4, θ_4 , respectively, as depicted in Fig. 2. The resonator can be analyzed using odd and even-mode analysis as the structure is symmetrical about A-A' plane. Fig. 2(a) and 2(b) show the even-mode and odd-mode equivalent circuits. Under odd-mode excitation there is a voltage null in the middle of the resonator structure, the equivalent circuit of which is shown by Fig. 2(b). It can be shown the admittances in the even-mode structure in Fig. 2(b) can be represented by

$$Y_{in}^e = Y_1 \left[\frac{Y_1^e + jY_1 \tan \theta_1}{Y_1 + jY_1^e \tan \theta_1} \right] \quad (1)$$

$$Y_1^e = Y_{01} \left[\frac{Y_2^e + jY_{01} \tan \theta_5}{Y_{01} + jY_2^e \tan \theta_5} \right] \quad (2)$$

$$Y_2^e = Y_2 \left[\frac{Y_3^e + jY_2 \tan \theta_2}{Y_2 + jY_3^e \tan \theta_2} \right] \quad (3)$$

$$Y_3^e = jY_3 \left[\frac{jY_3 \tan \theta_3 + Y_4 \tan \theta_4}{Y_3 - jY_4 \tan \theta_3 \tan \theta_4} \right] \quad (4)$$

Admittances in the odd-mode structure in Fig. 2(c) can be represented by

$$Y_{in}^o = Y_1 \left[\frac{Y_1^o + jY_1 \tan \theta_1}{Y_1 + jY_1^o \tan \theta_1} \right] \quad (5)$$

$$Y_1^o = Y_{01} \left[\frac{Y_2^o + jY_{01} \tan \theta_5}{Y_{01} + jY_2^o \tan \theta_5} \right] \quad (6)$$

$$Y_2^o = -jY_2 \cot \theta_2 \quad (7)$$

At resonance $Y_{in}^e = 0$ and $Y_{in}^o = 0$, so Eqn.(1) reduces to $Y_1^e = -jY_1 \tan \theta_1$, Eqn.(2) then simplifies to

$$Y_{01}(Y_1 \tan \theta_1 + Y_{01} \tan \theta_5)(Y_2 + jY_3^e \tan \theta_2) = Y_2(Y_3^e + jY_2 \tan \theta_2)(Y_{01} + Y_1 \tan \theta_1 \tan \theta_5) \quad (8)$$

Resonance frequency of the even-mode can then be determined from Eqn.(8), i.e. when $\tan \theta_1 \tan \theta_5 = 1/\beta_1$, where $\beta_1 = Y_1/Y_{01}$. When $\theta_1 = \theta_2 = \theta$ then $\theta(f_1) =$

$\tan^{-1}\sqrt{1/\beta_1}$ and $\theta(f_3) = \pi - \tan^{-1}\sqrt{1/\beta_1}$. Similarly, from Eqn. (8), $\beta_1 \tan \theta_1 + \tan \theta_5 = 0$. Electrical length of the resonator is sum of θ_1 and θ_5 . When $\theta_1 = \theta_5 = \theta$ then $\theta(f_2) = \pi/2$ and $\theta(f_4) = \pi$. Also from Eqn. (8), $\tan \theta_3 \tan \theta_4 - \beta_3 = 0$, where $\beta_3 = Y_3/Y_4$. When $\theta_3 = \theta_4 = \theta$ then $\theta(f_5) = \tan^{-1}\sqrt{\beta_3}$ and $\theta(f_6) = \pi - \tan^{-1}\sqrt{\beta_3}$. The odd-mode structure results in identical expressions at resonance frequency.

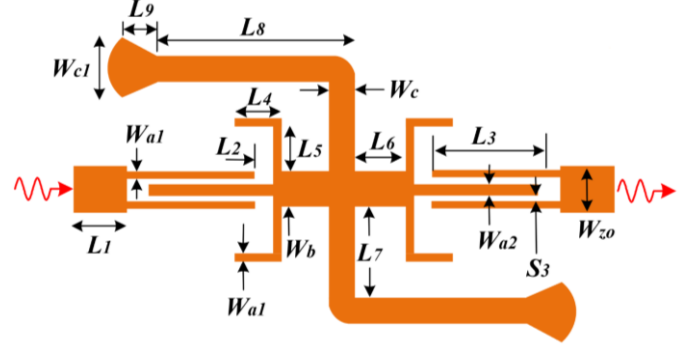


Fig. 1. Configuration of the proposed UWB bandpass filter.

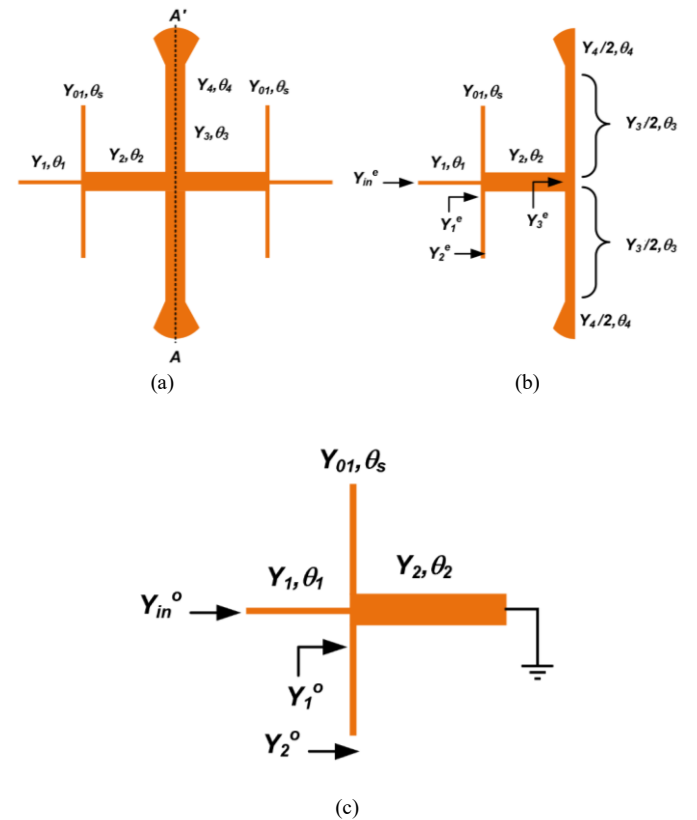


Fig.2. (a) Equivalent circuit model of the resonator structure, (b) even-mode circuit, and (c) odd-mode circuit model.

The fundamental and higher order resonant frequencies can be adjusted over a wide frequency range by modifying the admittance ratio (β) and the length ratio α defined as $\alpha = \theta_i/(\theta_i + \theta_{i+2})$ where $i = \text{integer}$. The analysis shows that different resonant modes can be combined to obtain a wider passband response, which is a function of α and β .

Assuming that the microstrip-lines are non-dispersive and line sections have equal phase velocity as $\alpha \propto f$, the various resonant frequencies normalized to the mode ratio of fourth to second are:

$$f_{1n} = 2(\tan^{-1}\sqrt{1/\beta_1})/\pi \quad (9)$$

$$f_{3n} = 2[1 - (\tan^{-1}\sqrt{1/\beta_1})/\pi] \quad (10)$$

$$f_{5n} = 2(\tan^{-1}\sqrt{\beta_3})/\pi \quad (11)$$

$$f_{6n} = 2[1 - (\tan^{-1}\sqrt{\beta_3})/\pi] \quad (12)$$

It is evident from the analysis that the six resonance modes contribute towards the passband of the filter. The mid-band second and fourth modes are static and have no effect on variation of the filter's bandwidth. Fig. 3 shows how the first, third, fifth and sixth modes vary as a function of the admittance ratio (β). When the admittance ratio is decreased, the frequency of the first and sixth modes increase however the frequency of the third and fifth modes decrease. The trajectories of the mode pairs third and sixth, and first and fifth converge at unity admittance ratio which corresponds to the minimum passband. The graph shows that the passband can be theoretically increased from the minimum to maximum by 52% by either reducing or increasing the admittance ratio. This analysis shows that by carefully choosing the admittance ratio it is possible to precisely control the 3-dB passband of the filter.

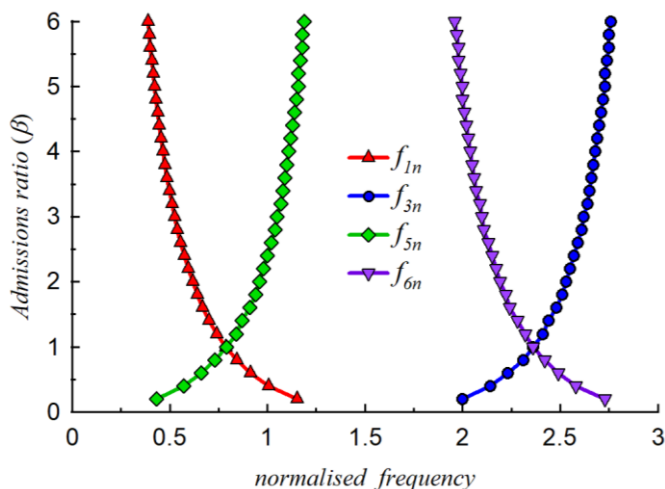


Fig.3. Normalized frequency of resonance modes as a function of impedance ratio.

III. DESIGN AND MEASURED RESULTS

The proposed UWB bandpass filter shown in Fig. 1 was fabricated using a dielectric substrate with thickness (h) of 0.794 mm, dielectric constant (ϵ_r) of 2.17, copper conductor thickness (t) of 35 μm , and loss-tangent ($\tan\delta$) of 0.0009. Simulation analyses using Advanced Design System (ADSTM) by Keysight Technologies was used to simulate and optimize the filter's performance. Optimized parameters are: $W_b = 0.95$ mm, $W_a = 0.23$ mm, $W_c = 1.19$ mm, $W_{c1} = 2.85$ mm, $W_{a2} = 0.23$ mm, $W_{z0} = 2.36$ mm, $L_1 = 5$ mm, $L_2 = 0.35$ mm, $L_3 = 6.1$ mm, $L_4 = 1.66$ mm, $L_5 = 1.43$ mm, $L_6 = 2.85$ mm, $L_7 = 3.57$ mm, $L_8 = 5.95$ mm, $L_9 = 1.28$ mm, and $S_3 = 0.23$ mm.

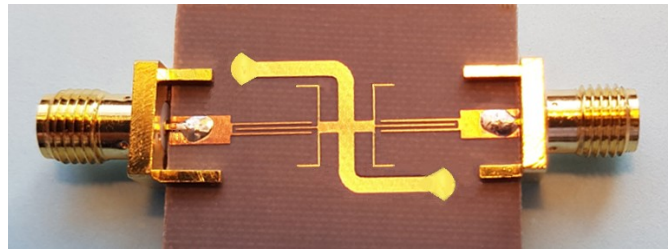


Fig.4. The fabricated UWB BPF.

The simulated and measured insertion-loss and return-loss of the fabricated filter in Fig. 4 are shown in Fig. 5. There is excellent correlation between the simulation and measured results. It is evident from the measured results the filter exhibits a quasi-elliptic response with an excellent in-band insertion-loss of 0.68 dB centered at 7.3 GHz with return-loss better than 17 dB. The two transmission zeros near the upper and lower cut-off frequencies of 3.1 GHz and 11.5 GHz, respectively, result in a filter with high selectivity. The combination of open-circuited stubs and interdigital coupled feedline in the filter structure creates notch responses at multiples of their fundamental frequency that suppress spurious responses. Hence, the out-of-band rejection is better than 30 dB over a very wideband between 12 to 26.35 GHz. The measured group-delay of the filter, shown in Fig. 6, is approximately flat and less than 0.5 ns within the passband. The total size of the filter is 13 mm \times 21 mm.

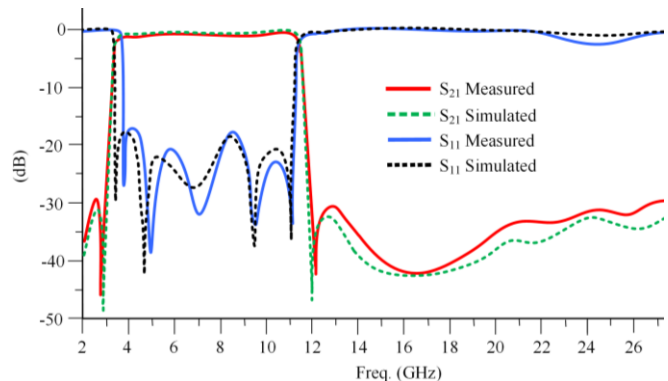


Fig. 5. Simulated and measured insertion-loss and return-loss response of the proposed UWB BPF.

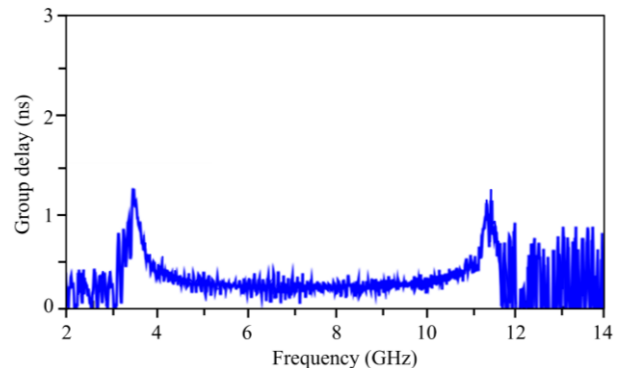


Fig. 6. The measured group delay of the proposed UWB BPF.

The performance of the proposed UWB filter is compared in Table 1 with similar type of filters reported to date. In references [2], [4], [16] and [17] the filters are fabricated on double-sided YBCO HTS films. One side of the HTS film is patterned into the filter circuit using high-precision processing of photolithography and ion etching. Unlike the proposed filter, which is realized on a standard dielectric substrate and operates at room temperature, the HTS filters need cryogenically cooling which makes this technology bulky and highly expensive. On the other hand, the UWB filter in [5] is based on two-layer substrate requiring metal vias which are necessary to create SIW. The UWB filter in [18] exhibits a marginally higher selectivity factor and fractional bandwidth than the proposed design however this is achieved by defecting the ground-plane with slots that are implemented under the input/output interdigital capacitors. It is evident that the proposed design offers advantages of: (i) lower passband loss than the HTS device in references [2] and [16]; (ii) much better return-loss than both HTS and Copper material devices; (iii) higher selectivity factor than HTS in references [4], [16] and [17]; (iv) lower insertion-loss, significantly better return-loss and higher out of band isolation than [18]; and (v) a significantly wider stopband than Copper and HTS designs. Compared to other UWB planar filters cited in Table 1 the proposed filter is etched on a single layer of standard dielectric substrate with no defected ground structure using a conventional fabrication technology.

TABLE 1
Comparison of the proposed UWB filter with recent publications

Ref.	Max. IL (dB)	Min. RL (dB)	$SF = \frac{\Delta f_{3dB}}{\Delta f_{30dB}}$	3dB FBW (%)	Size ($\lambda_g \times \lambda_g$)	Upper stopband (dB)	Material
[2]	0.75	10.7	0.910	122	1.53×0.45	<-30 (2 f_c)	HTS
[3]	0.80	12.0	0.650	95	0.89×0.96	<-30 (1.8 f_c)	Cu
[4]	0.42	15.2	0.877	125	1.57×1.18	<-30 (2.2 f_c)	HTS
[5]	1.00	14.0	0.682	110	N/A	<-30 (2.7 f_c)	Cu
[14]	0.80	16.5	0.685	101	0.24×0.19	<-30 (2.1 f_c)	Cu
[15]	1.60	11.5	0.790	110	0.51×0.54	<-20 (2.2 f_c)	Cu
[16]	1.20	12.0	0.800	98	0.64×0.32	<-20 (2.1 f_c)	HTS
[17]	0.42	15.2	0.877	125	1.57×1.32	<-20 (2.3 f_c)	HTS
[18]	1.40	11.1	0.902	117	0.51×0.37	<-20 (4.2 f_c)	Cu/DGS
This work	0.68	17.0	0.890	115	0.54×0.31	<-30 (3.6 f_c)	Cu

IL: max. insertion-loss; RL: min. return-loss; S.F.: selectivity factor; Δf_{3dB} , Δf_{30dB} : 3-dB bandwidth and 30-dB fractional bandwidth; 3-dB fractional bandwidth; λ_g : free space wavelength at center frequency; Cu: Copper; & DGS: Defected Ground Structure.

IV. CONCLUSION

The resonant modes generated by the unique z -shaped resonator can be controlled by adjusting the admittance of the filter structure to realize a UWB filter. The quasi-elliptic response is created with a pair of transmission zeros. The open-circuited stubs and the stepped impedance stubs at the input and output ports of the filter suppress unwanted spurious responses to widen the upper stopband. Tight electromagnetic coupling of the inter-digital feed mechanism is used to minimize the loss. The electrical characteristics of the proposed filter are comparable to expensive and bulky HTS filters. Moreover, the proposed filter is much cheaper to fabricate using standard dielectric substrate and it operates at room temperature. This performance of the proposed design was confirmed by experiment, and the measurement results are in good agreement with the simulations.

REFERENCES

- [1] FCC. revision of part 15 of the communications rules regarding ultra-wideband transmission systems. Washington DC. Tech. Rep. ET-Docket 98 – 153, FCC02-48; Feb. 2002.
- [2] T. Zhang, M. Tian, Z. Long, M. Qiao, and Z. Fu, “High-temperature superconducting multimode ring resonator ultrawideband bandpass filter,” *IEEE Microwave and Wireless Components Letters*, vol. 28, no. 8, August 2018, pp.663-665.
- [3] P. P. Shome, T. Khan, S. K. Koul, Y. M.M. Antar, “Compact UWB-to-C band reconfigurable filtenna based on elliptical monopole antenna integrated with bandpass filter for cognitive radio systems,” *IET Microwaves, Antennas & Propagation*, vol.14, Iss. 10, 2020, pp.1079-1088.
- [4] Z. Long, M. Tian, T. Zhang, M. Qiao, T. Wu, and Y. Lan, “High-temperature superconducting multimode dual-ring UWB bandpass filter,” *IEEE Transactions on Applied Superconductivity*, vol. 30, no. 2, March 2020.
- [5] M. M. Honari, R. Mirzavand, H. Saghlatoon, and P. Mousavi, “Two-layered substrate integrated waveguide filter for UWB applications,” *IEEE Microw. Wireless Compon. Lett.*, vol. 27, no. 7, Jul. 2017, pp. 633–635.
- [6] J. Sun, and G. Rui Li, “A balanced ultra-wideband bandpass filter based on H-type sandwich slotline,” *International Journal of RF and Microwave Computer-Aided Engineering*, vol. 31, Issue 5, 2021, 1-7.
- [7] X. Xia, F. Chen, X. Cheng, and X. Deng, “A compact ultra-wideband bandpass filter with good selectivity based on interdigital coupled-line,” *International Journal of RF and Microwave Computer-Aided Engineering*, vol. 28, issue 9, Nov.2018, pp. 1-7.
- [8] P. Kumari, M. Pal, P. Sarkar, and R. Ghatak, “Compact UWB bandpass filter with dual-notch bands using asymmetric tri-section stepped impedance resonator,” *International Journal of RF and Microwave Computer-Aided Engineering*, vol. 28, Issue 6, 2018, 1-8.
- [9] H. Wang, Y. Y. Zheng, W. Kang, C. Miao, and W. Wu, “UWB bandpass filter with novel structure and super compact size,” *Electron Lett.*, vol. 48, 2012, pp. 1068–1069.
- [10] W. Feng, L. W. Tao, S. X. Wei, H. Q. Lin, “Compact UWB bandpass filter with triple-notched bands using triple-mode stepped impedance resonator,” *IEEE Microwave and Wireless Components Letters*. vol. 22, no.10, 2012, pp. 512- 514.
- [11] F. Wei, Q. Y. Wu, X. W. Shi and L. Chen, “Compact UWB bandpass filter with dual notched bands based on SCRLH resonator,” *IEEE Microwave and Wireless Components Letters*, vol.21, no.1, Jan. 2011, pp.28-30.
- [12] L. Zhu, S. Sun, and W. Menzel, “Ultra-wideband (UWB) bandpass filters using multiple-mode resonator,” *IEEE Microwave and Wireless Components Letters*, vol. 15, no. 11, Nov. 2005, pp. 796-798.
- [13] Q.-X. Chu, X.-H. Wu, and X.-K. Tian, “Novel UWB bandpass filter using stub-loaded multiple-mode resonator,” *IEEE Microwave and Wireless Components Letters*, vol. 21, no. 8, Aug. 2011, pp. 403-405.
- [14] S.-W. Lan, M.-H. Weng, C.-Y. Hung, and S.-J. Chang, “Design of a compact ultra-wideband bandpass filter with an extremely broad stopband region,” *IEEE Microw. Wireless Compon. Lett.*, vol. 26, no. 6, Jun. 2016, pp. 392–394.
- [15] C. Zhou, P. Guo, K. Zhou, and W. Wu, “Design of a compact UWB filter with high selectivity and superwide stopband,” *IEEE Microw. Wireless Compon. Lett.*, vol. 27, no. 7, Jul. 2017, pp. 636–638.
- [16] X. Xia, X. Cheng, F. Chen and X. Deng, “Compact UWB bandpass filter with sharp roll-off using APCL structure,” *Electronics Letters*, vol. 54, no. 13, 2018, pp. 837–839.
- [17] Z. Long, M. Tian, T. Zhang, M. Qiao, R. Wu, and Y. Lan, “High-temperature superconducting multimode,” *IEEE Transactions on Applied Superconductivity*, vol. 30, no. 2, March 2020, pp. 1-4.
- [18] X.-H. Wu, Q.-X. Chu, X.-K. Tian, and X. Ouyang, “Quintuple-mode UWB bandpass filter with sharp roll-off and super-wide upper stopband,” *IEEE Microw. Wireless Compon. Lett.*, vol. 21, no. 12, Dec. 2011, pp. 661-663.